



HAL
open science

Technical economic analysis of PV-driven electricity and cold cogeneration systems using Particle Swarm Optimization algorithm

Antoine Perrigot, Maxime Perier-Muzet, Pascal Ortega, Driss Stitou

► To cite this version:

Antoine Perrigot, Maxime Perier-Muzet, Pascal Ortega, Driss Stitou. Technical economic analysis of PV-driven electricity and cold cogeneration systems using Particle Swarm Optimization algorithm. *Energy*, 2020, 211, pp.119009. <10.1016/j.energy.2020.119009>. <hal-02972731>

HAL Id: hal-02972731

<https://hal.science/hal-02972731v1>

Submitted on 20 Oct 2020

HAL is a multi-disciplinary open access archive for the deposit and dissemination of scientific research documents, whether they are published or not. The documents may come from teaching and research institutions in France or abroad, or from public or private research centers.

L'archive ouverte pluridisciplinaire HAL, est destinée au dépôt et à la diffusion de documents scientifiques de niveau recherche, publiés ou non, émanant des établissements d'enseignement et de recherche français ou étrangers, des laboratoires publics ou privés.



HAL Authorization

Technical economic analysis of PV-driven electricity and cold cogeneration systems using Particle Swarm Optimization algorithm

PERRIGOT Antoine ^{a,*}, PERIER-MUZET Maxime ^a, ORTEGA Pascal ^b, STITOU Driss ^a

^a CNRS-PROMES laboratory, Tecnosud, Rambla de la thermodynamique, 66100 Perpignan, France

^b GEPASUD Laboratory, University of French Polynesia, BP 6570, 98702 Tahiti, French Polynesia

* Corresponding author : antoine.perrigot@promes.cnrs.fr

Keywords : cogeneration, cold, electricity, thermochemical process, hydrogen, particle swarm optimization

Abstract

Three different studies are presented in this paper. As a first step, a Particle Swarm Optimization (PSO) algorithm is used to optimize a prototype of cold/electricity cogeneration designed to be disconnected from the grid and implanted in an insular tropical region where a high need of cold and electricity is required. The electricity is provided by solar photovoltaic panels and the electrical energy in excess is stored in the form of hydrogen thanks to an electrolyzer. When a lack of electricity occurs a fuel cell provides the missing electricity by using the stored hydrogen. An electrically driven heat pump is also used to produce and cover the cold needs. Finally, in order to increase the overall efficiency of this electricity/cold cogeneration system, the low-grade waste heat generated by the different components of the system, mostly the electrolyzer and the fuel cell, is recovered and upgraded by a thermochemical reactor enabling a further cold production. The thermochemical reactor assists the heat pump for the cold supply, decreasing thus the electricity consumption. Such a prototype is intended to be built in Tahiti during the RECIF project. The PSO algorithm has been implemented and results are promising because component's size is reasonable, and the driving strategy is consistent while both demands are always satisfied. In a second study, the same PSO algorithm has been used to perform an analysis and identify a general shape of load profiles for which it become interesting, from an economic point of view, to store electricity into hydrogen instead of electrochemical batteries when the cold production is only handled by a heat pump. This study has shown that the more electricity is consumed at night, the more it is interesting to use hydrogen. Finally, the algorithm has been used to see the evolution of the economic interest when a thermochemical system is added. This study has been carried out considering a storage into hydrogen and an exploitation of the low-grade heat by a thermochemical unit to enable a further cold production. The economic interest of a thermochemical system has not been proven by this study, that is why further considerations must be considered in order to justify its use as ecological impacts for example.

Greek symbols

ΔH_r	Enthalpy of reaction (J.mol ⁻¹)
ΔH_{vap}	Enthalpy of vaporization (J.mol ⁻¹)
ν	Stoichiometric coefficient
η	Efficiency
ΔE_{H2}	Variation of energy inside the H ₂ tank (J)
ΔE_{cold}	Variation of energy inside the "cold" tank

Acronyms, subscripts and superscripts

COP	Coefficient of performance
GHI	Global horizontal irradiance
TCS	Thermochemical system
HP	Heat pump
PV	Photovoltaic
EL	Electrolyzer
FC	Fuel cell
H2	Hydrogen

Names and variables

\dot{W}	Electrical power (W)
\dot{Q}	Thermal power (W)
A_{pv}	Area of PV panels (m ²)
N_{gas}	Size of the gas storage for the TCS (kWh)
N_{H2}	Size of the hydrogen storage (kWh)
S_{poor}	Salt poor in gas
S_{rich}	Salt rich in gas
C_{cap}	Capital cost
$C_{o\&m}$	Operation and maintenance cost
C_{rep}	replacement cost

1. Introduction

In the context of reduction of greenhouse gases emissions, renewable energies will have a bright future if storage solutions are found in order to overcome the intermittence of such means of energy production. A solution to store electricity that seems quite promising is the association of an electrolyzer and a fuel cell in order to store electrical energy in the form of hydrogen. The greatest impediment of such a storage system lies in its low efficiency. Indeed, the energy efficiency of a conventional alkaline water electrolysis is around 70 % and the one of proton exchange membrane (PEM) fuel cell system is generally between 40-60% energy efficient [1]. Assuming no losses in the hydrogen storage the global efficiency is around 35%. This means that a major amount of inlet energy is released into low-grade heat energy (70-80 °C). To increase this overall efficiency, some authors propose to directly use this low-grade heat to assist the hot water production or to directly heat a room [2], [3]. Another track is to use this heat to power an organic Rankine cycle and thus produce a mechanical work [4] and then more electricity. The heat could also be used with an absorption chiller in order to produce cold [5]–[7]. Finally, a trigeneration system with heat retrieving from the fuel cell can be designed and has already been widely studied as in [8]–[16]. The system introduced in this article also intends to use the low-grade heat in order to produce cold by implementing a thermochemical sorption process. This thermochemical process, called adsorption, is based on a reversible chemical reaction between a solid reactive and a gas, allows to store thermal energy in a chemical potential form, which subsequently makes it possible to produce cold. This process is well documented and has already been implemented for several applications, such as solar air conditioning, solar ice making or deep-freezing [17]–[21].

In this context, a potentially interesting system suitable for regions with a high need of cold production and which are poorly interconnected to the electricity grid is under development. An experimental demonstration in French Polynesia is scheduled by 2022 as part of the RECIF project funded by the French national research agency (ANR). This location has been chosen because the high ambient temperatures and humidity requires all over the year a large amount of energy to meet the cold needs. Indeed, the cold production represents approximately 36% of the total energy consumption for a typical household in French Polynesia [22]. In addition to this assessment, French Polynesia is facing a large issue of primary energy importation : 94 % of the primary energy consumed on-site is imported [23]. Today, despite a high average global solar horizontal irradiation about 5.8 kWh/m²/day (compared to 3.6 kWh/m²/day in Paris for example), renewable energies count only for 6.4 % of the total primary energy consumption in French Polynesia and this renewable energy production is mainly located in Tahiti with hydroelectric power stations. The other islands are strongly dependent on imported fossil fuels, inducing a significant impact on ecosystems. To decrease these ecological impacts, solar energy has to be more exploited. Photovoltaic electricity production, coupled with efficient storage systems, seems to be a relevant solution to address these challenges.

An isolated cogeneration system includes several components and has to implement storage technologies in order to always fulfill demands. Optimizing such a system remains quite a challenge because a non-convex optimization problem with a lot of optimization variables must be tackled down. In addition, a control strategy of this system must be found in order to always ensure the supply of the demands. Indeed, several storage units coexist in the system which involve a choice at each step time to manage efficiently the energy within the system. The optimization algorithm should then be able to find a solution which simultaneously optimize the size of each component and a control strategy under a given set of constraints. Nevertheless, because there is no purpose to find the optimal solution in the mathematical sense of the term, evolutionary search algorithms can be use. This new branch of optimization, born in the late quarter of the twentieth century [24], use a population of several agents (or particles) that travel through the space of possible solutions. These methods do not require any gradient information and can tackle problems involving a high number of variables to optimize under many constraints. However, as said before, the obtained solution is a sub-optimal solution of the problem and not the optimal one in the mathematical sense of the term because these algorithms are metaheuristic approaches and do not provide the certainty that the best solution has been found. Two main strategies exist in the field of evolutionary search algorithm. The first ones are called Genetic Algorithms (GA) and have been developed by Holland et al. in [25]. This algorithm uses a population submitted to random mutations. From these mutations, a new offspring is designed and only the best agents of the population are kept for the next generation. The second most known way to design an evolutionary search algorithm is to have a population of particles and to make this population move in the search space according to the best particle in the population. This method is called Particle Swarm Optimization (PSO) and has been developed by Eberhart and Kennedy in 1995 [26].

The particularity of these two algorithms (GA and PSO) is that there have been inspired by the environment. The first one has drawn its inspiration into the Darwin theory and the second one in the social behavior of bird flocking. More recently, the two methods have been interbred to create, among others, the PSO-DV algorithm (Particle Swarm Optimization with a Differential operator in the Velocity update) [27] which is used for the studies presented in this paper. In this algorithm a random mutation is applied to compute the new velocity of each particle of the swarm to increase the search capabilities.

This algorithm has been used because of its simplicity of implementation and its satisfactory results obtained in a short computation time (a few minutes for 14 days simulation). A result is said satisfactory if both demands are always satisfied and if energy storage levels return to their original states after the considered period. Even if metaheuristic algorithm such as the PSO algorithm does not provide the best solution in the mathematical sense of the term, an approximate solution is nevertheless satisfactory for the critical thermo-economic analysis and the impacts of the building energy load profiles that is made in this article. In addition Particle Swarm Optimization has already widely been used for energy management in complex systems [28]–[32].

This PSO algorithm, implemented in *Matlab*, is used in 3 different studies in this paper. First, using real data from an instrumented building in Tahiti, the cogeneration system under development in the RECIF project is optimized in order to have a rough idea of the size of the different components and define a possible way to manage the cogeneration system in order to meet both electricity and cold demands. Such an optimization is not new in the literature, but this casts the light on the feasibility of this new cogeneration system detailed below in this paper. The second study uses different cold and electricity load profiles to see the impacts on the economic interest to use hydrogen instead of electrochemical batteries to store electricity when the cold production is only handled by a heat pump. This part brings a greater understanding on the question of electricity storage with hydrogen or with electrochemical batteries to the literature. Finally, using the same set of load profiles as in the previous study, the impacts on the economic interest of a thermochemical unit in a system where hydrogen is used to store electricity is studied. This study also tends to define which is the appropriate energy distribution in the load profiles that minimizes the cost of such an installation when low-grade heat is recovered and valorized through a thermochemical sorption system to produce cold.

This paper is structured as follows: a description of the prototype under development is first provided in section 2. The following section deal with the presentation and description of the PSO algorithm and section 4 presents a case study of a set of data for a residential building in Hawaii. Two case studies are presented in section 5 in order to assess the economic interest of such a system as a function of load profiles. Finally, a conclusion is reached in the last section.

2. System description

In the system depicted in *Figure 1*, the energy production is handled by photovoltaic panels. The electricity produced during the day is directly used for the electrical needs of the building. Cold requirements are fulfilled thanks to an electrically driven heat pump. When there is an excess of electricity regarding the direct consumption, the excess electricity is stored in hydrogen form: an electrolyzer is used to produce hydrogen by the decomposition of water. If there is a lack of electricity, occurring during cloudy days or the night-time period, the opposite reaction takes place in the fuel cell, which produce electricity and water by consuming the stored hydrogen and oxygen of air.

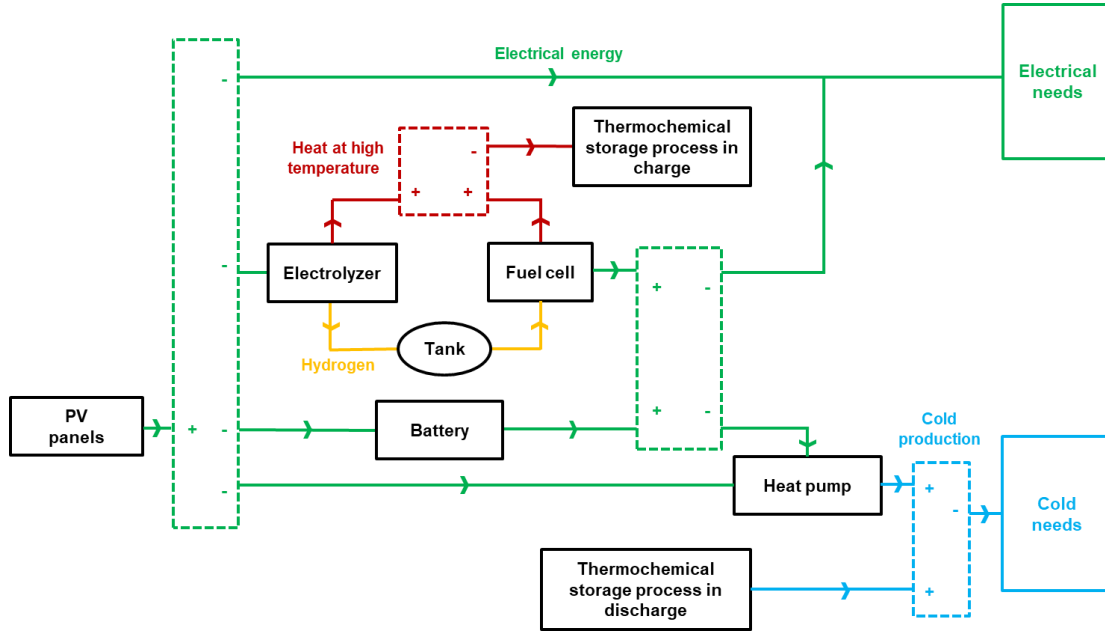


Figure 1: Scheme of the system architecture combining a hydrogen-based storage of electricity with an electrolyzer, a fuel cell and two thermochemical reactors.

A thermochemical system is furthermore implemented in order to store and produce cold by recovering the waste heat that is released by these two last components (electrolyzer and fuel cell). This thermochemical storage system decreases the electrical energy that is consumed by the heat pump and increase the overall energy by retrieving the low-grade heat. As it will be seen in the following section, two thermochemical reactors have to be used in order to always have one ready to exploit the low-grade heat generated either by the electrolyzer or the fuel cell.

2.1. Principle of a solid/gas thermochemical sorption process

A solid/gas chemisorption process is based on the implementation of a reversible chemical reaction between a solid and a refrigerant gas, which can be described with the following equation:



Where S_{poor} is the sorbent (a salt) poor in gas, S_{rich} is the salt rich in gas and $\Delta H_{r, TCS}$ is the enthalpy of reaction per mole of gas involved. Ammonia is used as a refrigerant gas in the system described above.

By coupling such a solid/gas reaction with a liquid/gas phase change of the same gas, a sorption cooling process can be designed. The implementation of a thermochemical cooling process requires then the linking of two components: a reactor where the chemical reaction takes place and an evaporator or condenser in which the evaporation or condensation of the reactive gas happens, according the following reaction:



ΔH_{vap} is the enthalpy of vaporization. Generally, this basic cooling sorption process operates in two different stages as depicted in Figure 2. During the charging step, the endothermic reaction following the right-to-left direction in equation (1) occurs. By supplying low-grade heat released by the electrolyzer or the fuel cell to the reactor, a decomposition reaction of the rich salt is initiated and makes the gas desorb from the reactor. The desorbed gas condenses in the condenser at ambient temperature and is stored in its liquid form in a tank. When all the "rich salt" has been decomposed and transformed into "poor salt", then the synthesis phase or discharging phase can take place: the reactor is cooled down and maintained at ambient temperature. This cooling down makes the "poor salt" reabsorb the reactive gas and induces the boiling of the liquid in the evaporator thus producing a cooling effect below the ambient temperature.

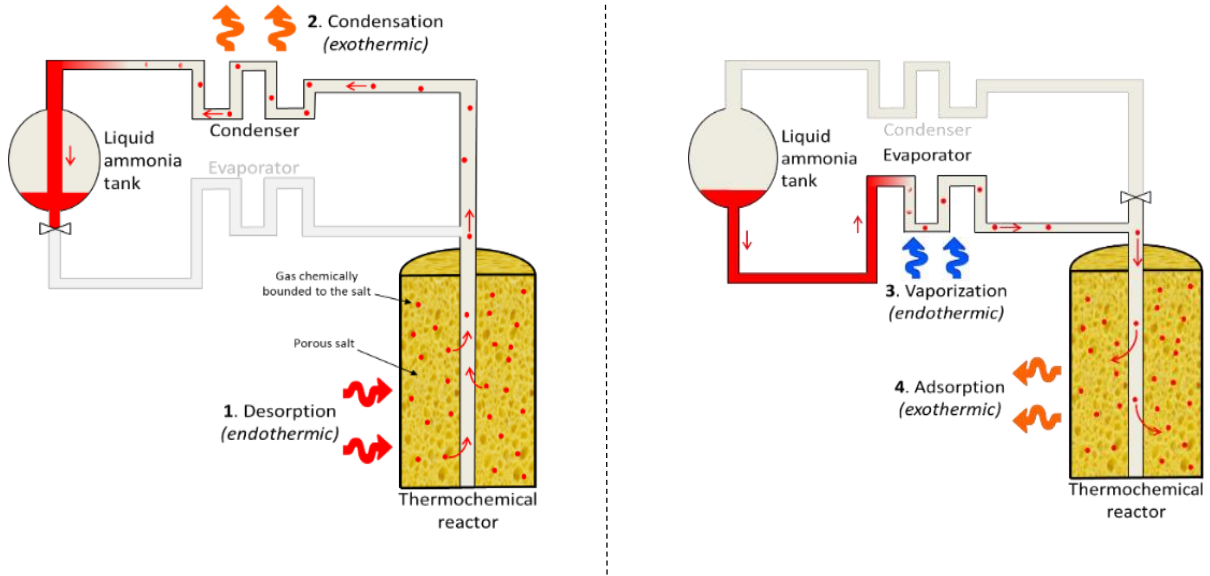


Figure 2: Scheme of the thermochemical system during the decomposition (charging step) on the left and the cold production (discharging step) on the right.

The model that is considered in the algorithm for this thermochemical storage process is a streamlined approach. It is assumed that for each $\Delta H_{r, TCS}$ of thermal energy amount brought to the reactor, one mole of reactive gas is generated according to equation (1) and stored in liquid form in the reservoir after having condensed. When a cold production is needed, it is considered that each mole of liquid, which is withdrawn from the tank, evaporated at the evaporator and absorbed chemically by the salt into the reactor, enables a cold energy production of ΔH_{vap} at the evaporator. Finally, this energy efficiency of the thermochemical system is measured throughout a coefficient of performance (COP) which is defined in first approximation as the ratio of the involved enthalpies $\Delta H_{vap}/\Delta H_{r, TCS}$. For the sake of simplicity, it is assumed that this COP is constant and equal to 0.3. This value has been extracted from [33] which present a state-of-art of experimental research about thermochemical energy storage.

As it is not possible to have the charging step occurring at the same time as the discharging one and as it is desirable to maximize the efficiency of the whole system, it is necessary to implement two reactors: one in storing phase ready to absorb the released heat and another one ready for a cold production. The two thermochemical systems are exchanged when the one in decomposition phase has reached its maximum amount of storage capacity, which depends on the reactive salt amount contained in the reactor. A more deeply explanation of the principle of solid/gas thermochemical sorption is made in [19].

2.2. Components models description

As said before, the main idea of this article is to have a global overview of the way the system could work thanks to a pre-sizing process which give access to the different component sizes and a control strategy to activate/deactivate them depending on the solar resource and the energy requirement of the building. For this purpose, the energy and power behavior of each component of the system is modeled in a simplified way assuming characteristic efficiency values.

- **PV panels** - A constant overall PV system efficiency of $\eta_{pv}=0.15$ by considering monocrystalline silicon modules. The Global Horizontal Irradiance (GHI) is used to compute the electric power meaning that PV panels are supposed to be installed horizontally, which corresponds approximately to the installation site latitude. The panel surface is A_{PV} . The electrical power W_{pv} which can be delivered by the photovoltaic panels is then expressed by the following equation:

$$\dot{W}_{PV}(t) = \eta_{PV} \cdot A_{PV} \cdot GHI(t) \quad (3)$$

- **Mechanical Heat pump** - A constant Coefficient of Performance $COP_{hp}=3.5$ has been considered. The COP is defined as the ration between the produced cold and the consumed electricity. To compute the produced cold the following formula can be used :

$$\dot{Q}_{hp} = \dot{W}_{hp} \cdot COP_{hp} \quad (4)$$

- **Electrolyzer** – A constant efficiency of $\eta_{el} = 0.7$ is considered and the released heat can be computed with:

$$\dot{Q}_{el} = (1 - \eta_{el}) \cdot \dot{W}_{el} \quad (5)$$

- **Fuel cell** - A constant efficiency of $\eta_{fc}=0.5$ is taken and the heat released can be computed with:

$$\dot{Q}_{fc} = \frac{(1 - \eta_{fc})}{\eta_{fc}} \cdot \dot{W}_{fc} \quad (6)$$

- **Electricity storage evolution** - Between each time interval Δt the variation of stored energy in the hydrogen tank can be computed thanks to the following equation, taking into account the energy balance at inlet (hydrogen produced by the electrolyzer) and at the outlet (hydrogen consumed by the fuel cell) of the tank. The difference between these two quantities multiplied by the time interval gives the evolution of the hydrogen stock in term of stored energy:

$$\Delta E_{H2} = \left(\eta_{el} \cdot \dot{W}_{el}(t) - \frac{\dot{W}_{fc}(t)}{\eta_{fc}} \right) \cdot \Delta t \quad (7)$$

- **Cold storage evolution** – Similarly to the hydrogen evolution, the variation of the cold energy stored in the ammonia tank of the thermochemical unit can be computed from an energy balance at each time step with the following equation:

$$\Delta E_{cold} = \left(\left((1 - \eta_{el}) \cdot \dot{W}_{el}(t) + \frac{1 - \eta_{fc}}{\eta_{fc}} \cdot \dot{W}_{fc}(t) \right) \cdot COP_{tcs} - \dot{W}_{tcs}(t) \right) \cdot \Delta t \quad (8)$$

3. Particle Swarm Optimization algorithm

Particle Swarm Optimization (PSO) is a multi-agent parallel search technique where all the agents can communicate to give their best personal score. The PSO procedure is shown on *Figure 3*. In this algorithm, each particle of the swarm has a position which represents a possible solution to the optimization problem.

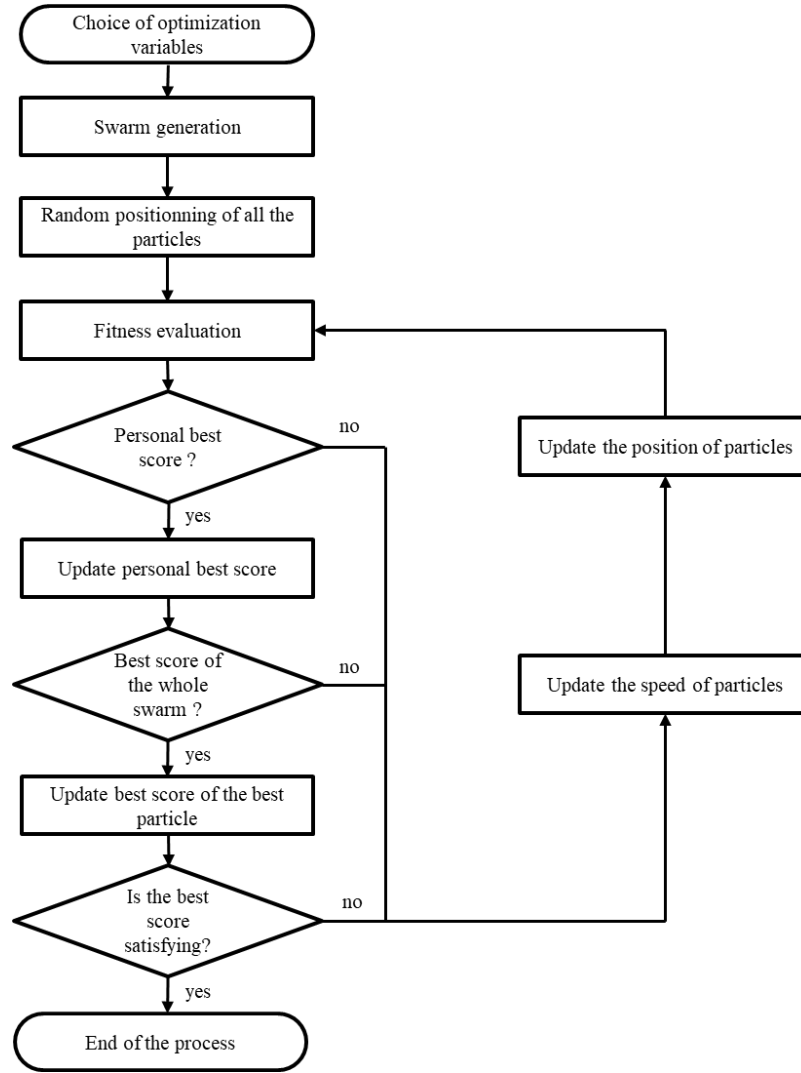


Figure 3: Procedure of the PSO algorithm.

To start the process, a random position and velocity are assigned to each particle into the search space. At each step, each particle of the swarm is evaluated according to a fitness function that gives a score to the particle. The convergence of this algorithm is insured through the way the speed is modified at each step. Indeed, three parameters are considered for the displacement of each particle:

- The current velocity of the particle: *the inertia term*
- The best previous position of this particle: *the cognitive term*
- The best position of the best particle of the swarm: *the social term*

The update of the particle velocity can be expressed by the following equation:

$$\vec{V}_i(t+1) = \omega \cdot \vec{V}_i(t) + C_1 \cdot \Phi_1 \cdot (\vec{P}_{best} - \vec{X}_i(t)) + C_2 \cdot \Phi_2 \cdot (\vec{G}_{best} - \vec{X}_i(t)) \quad (9)$$

Where ω is the inertia factor taken in $[0; 1]$, C_1 and C_2 are respectively the self-confidence factor and the swarm-confidence factor. C_1 contributes to the exploration of the search space by the particle itself when C_2 encourage the particle to go towards the actual extremum. Φ_1 and Φ_2 are two random numbers uniformly distributed in $[0; 1]$ which increase the search capability of the swarm by giving a random aspect to each particle of the swarm.

In order to design a PSO algorithm, two things must be done: design a fitness function which considers all the optimization criteria and choose with relevancy the optimization variables. These two points are treated below.

3.1. Fitness function

The goal of the fitness function is to evaluate a particle on different relevant criteria. Each criterion can initially be asked as a question: are cold and electricity demands always satisfied? Do levels of energy storages return to their initial states? How much does the system cost? Then, each of these questions must be translated into equations in order to give a score for each criterion. Thereafter, these scores have to be normalized in order to be able to compare them.

The system being disconnected from the grid, the two most important criteria are the respect of cold and electricity demands. For the normalization of these two scores, the maximum between the production and the consumption has been used at each step. The final normalized scores for the respect of demands in electricity and cold have been constructed by taking the mean value of the normalized scores at each step time.

The normalized scores at each step are calculated as follows:

$$Score_{electrical\ demand} = mean \left(\frac{|\dot{W}_{pv}(t) + \dot{W}_{fc}(t) - \dot{W}_{load}(t) - \dot{W}_{el}(t) - \dot{W}_{hp}(t)|}{\max[\dot{W}_{pv}(t) + \dot{W}_{fc}(t); \dot{W}_{load}(t) + \dot{W}_{el}(t) + \dot{W}_{hp}(t)]} \right) \quad (10)$$

$$Score_{cold\ demand} = mean \left(\frac{|\dot{W}_{hp}(t) \cdot COP_{hp} + \dot{Q}_{tcs1}(t) + \dot{Q}_{tcs2}(t) - \dot{Q}_{cold}(t)|}{\max[\dot{W}_{hp}(t) \cdot COP_{hp} + \dot{Q}_{tcs1}(t) + \dot{Q}_{tcs2}(t); \dot{Q}_{cold}(t)]} \right) \quad (11)$$

Others important criteria concern the return to the initial state for the two storages over a given considered period. As explained before, at each step time Δt the hydrogen variation in the tank is determined thanks to the equation (7). The energy difference between the initial time and the end of the considered period can be computed and normalized thanks to the maximum amount of energy stored during the simulation :

$$Score_{H_2\ stock} = \frac{\sum_{period} \left(\eta_{el} \cdot \dot{W}_{el}(t) - \frac{\dot{W}_{fc}(t)}{\eta_{fc}} \right) \cdot \Delta t}{maximum\ stored\ energy} \quad (12)$$

For the cold storage a similar reasoning can be applied based on equation (8):

$$Score_{cold\ stock} = \frac{\sum_{period} \left(\left((1 - \eta_{el}) \cdot \dot{W}_{el}(t) + \frac{1 - \eta_{fc}}{\eta_{fc}} \cdot \dot{W}_{fc}(t) \right) \cdot COP_{tcs} - \dot{Q}_{tsc}(t) \right) \cdot \Delta t}{maximum\ stored\ energy} \quad (13)$$

Other technical or economic criteria can be added such as the size or the cost of the components in order to minimize it. Indeed, a relevant criterion is the life cycle cost (LCC). Its minimization enables to directly optimize the size of the different components of the whole system considering an economic criterion. C_{cap} represents the capital cost, $C_{O\&M}$ the operation and maintenance cost and C_{rep} the replacement cost. The LCC can be computed as follows:

$$LCC = C_{cap} + C_{O\&M} + C_{rep} \quad (14)$$

The normalization of this last criterion is not obvious. Maximum sizes for each component have to be defined in order to have a maximum value of the LCC. The following values have then been considered :

- PV area, H_2 and NH_3 stocks are optimization variables. Intervals have been defined to restrict the range of possible values. The upper limit of the interval has been considered for the normalization of the LCC.
- Considering that the electrolyzer must be able to consume all the electricity produced by the photovoltaic panels when there is no electric demand, the maximum value of \dot{W}_{el} has been computed by taking into account the maximum irradiation and the largest required area of photovoltaic panels.
- The maximum size of the fuel cell has been computed considering that it should be able to supply electricity to the load even if there is no sun.

- The maximum sizes of the thermochemical systems and of the heat pump have been computed by considering that in the worst case, these components must supply all the cold demand of the building.

Finally, a final criterion has also been added to prevent the system to exchange too often the two thermochemical systems because a thermochemical reactor has a high thermal inertia. This criterion has been normalized using the maximum number of times the system could exchange its reactors.

Once each score has been normalized, some weights have been applied to each score to give more importance to certain criterion than others. Starting with a unitary weight assigned to each score, the algorithm was not able to satisfy both demands, therefore weights of the electrical and cold demands have been increased. Once both demands have been satisfied, the weights assigned to the storage has been risen in order to make them return to their initial states at the end of the simulated period. At last, the LLC weight have been put to its maximum value to minimize the cost of the whole system while still satisfying the other criteria. There are obviously a lot of sets of weight that gives satisfactory results, but the following table sums up some correct values :

Score	Weight
LCC	10
Electrical demand	4
Cold demand	3
Return to initial value for H ₂ stock	3
Return to initial value for NH ₃ stock	2
Reactor exchange	1

Table 1 : Weights of the different scores for the fitness function

3.2. Optimization variables

A PSO algorithm can optimize at the same time the size of the components and the way the system can be driven if relevant optimization variables are chosen. Three optimization variables are directly related to the size of the system components:

- A_{pv} : total area of solar panel in m².
- N_{gas} : size of the storage of the reactive gas of the thermochemical unit in kWh_{cold}. The size of the storage in m³ can be obtained using the enthalpy of vaporization and the molar mass of the gas.
- N_{H2} : size of the storage of hydrogen in kWh_{elec}. The size of the storage in m³ can also be obtained using the energetic density of hydrogen.

In order to control the system new optimization variables α in [0; 1] must be created. Theses variables represent the dispatching of cold production between the heat pump and the thermochemical storage ($\alpha = 0$ means that all the cold production is handled by the heat pump). If the simulation is running for a whole day with a step time of one hour each particle will provide 24 values for α which correspond to a possible way to manage our system during the day.

At each iteration of the algorithm, optimization variables are recovered, and the different powers at stake in the system are computed as shown in *Figure 4*. The size of the system components that were not put as optimization variables can be obtained with the presented algorithm.

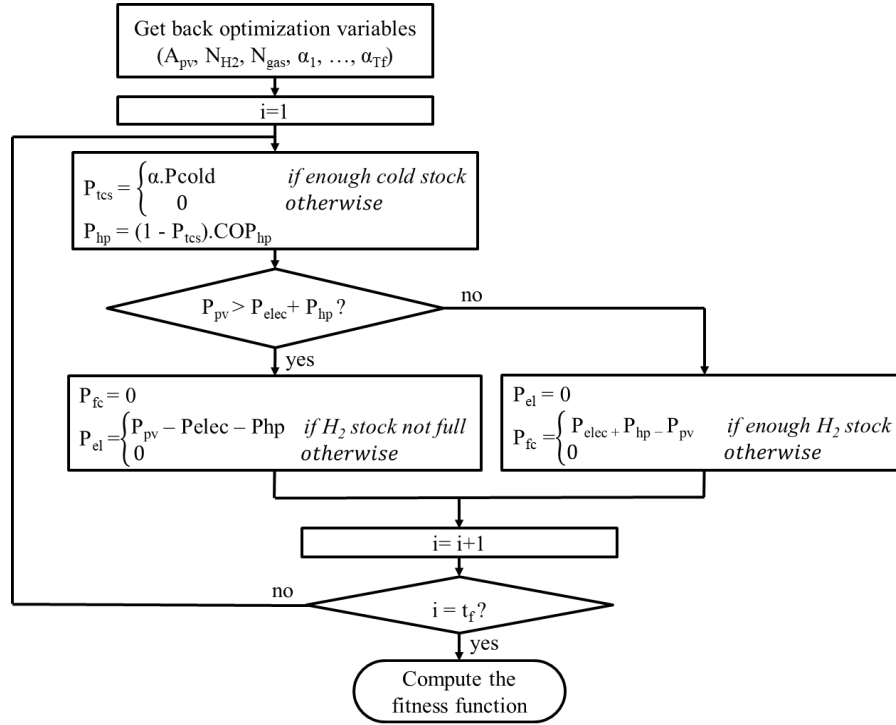


Figure 4: Pseudo-code to compute all the powers at stake in the system from the values of the optimization variables.

4. Case study

This part describes the procedure used to apply the algorithm and the results given by the optimization for a given set of resource data and energy demand profiles of a building.

4.1. Data presentation

A measurement campaign has been started in Tahiti for the RECIF project and nevertheless these data are not available yet for a long period. Therefore the following study uses simulated data about a residential building in Hawaii over 11 months (February to December). These data are available online [34] as well as a description of the simulated residential building [35]. Hawaii and Tahiti have roughly the same climate except that the seasons are reversed. An overview of the data is shown on *Figure 5*. The consumed energies over the year of the considered building are about 13MWh for electricity and 9.5MWh for the cold which represent the consumption of 3 or 4 households.

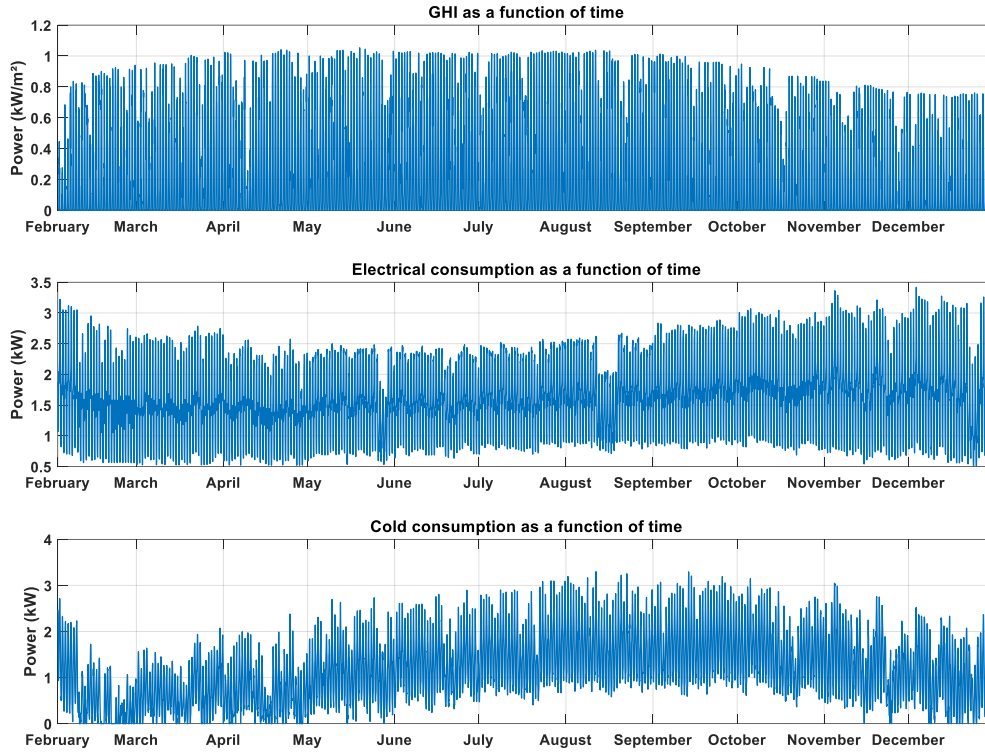


Figure 5 : Simulated data for a residential building in Hawaii (from [34], [35])

The different component costs taken from the literature [36-39] that have been considered for the optimization are presented in *Table 2*. Concerning the cost of the thermochemical unit, one must keep in mind that such systems are not yet industrially developed and are thus quite expensive. The cost could be significantly reduced in the future if the manufacturers develop this thermochemical storage system. Nevertheless, this cost is an approximate cost estimated from the past experience of the PROMES laboratory. It is also essential to keep in mind that the results presented in the next section are highly dependent on the considered costs.

Component	Initial cost	Maintenance cost	Replacement cost	Lifetime
Photovoltaic panels	250€/m ²	7€/m ² /y	200€/m ²	+25y
Heat pump	500€/kW	100€/kW/y	400€/kW	+25y
Electrolyzer	1500€/kW	80€/kW/y	1300€/kW	10y
Fuel cell	4000€/kW	200€/kW/y	2000€/kW	8y
Hydrogen storage	30€/kWh	5€/kWh/y	25€/kWh	+25y
Electrochemical batteries	400€/kWh	10€/kWh/y	300€/kWh	4y
Thermochemical system	500€/kWh	15€/kWh/y	400€/kWh	+25y

Table 2: Components costs considered for the economic assessment.

4.2. Finding the worst scenario to size the system

The main interest of the system lies in its ability to provide electricity and cold for buildings that are isolated from the microgrid. The demands will then be satisfied only if the system is sized according to the worst scenario of the year. This scenario is extracted from the data over a given period chosen by the user. This period must be chosen carefully as it corresponds to the time after which each storage should have retrieved its initial state. In addition, it is important for the user to have a rough idea of the number of occurrences of this worst scenario during the year. Indeed, it would be expensive to build a system sized according to one day occurring

once a decade. To find the worst scenario, the following indicator (15) that compares the solar energy resource to the whole energy consumed by the building has been used :

$$Ratio(period) = \frac{Ressources}{Consumptions} = \frac{\sum_{period} GHI}{\sum_{period} (Electricity + Cold)} \quad (15)$$

Once the storage period chosen, ranging from 1 to 14 days, this ratio is computed over the year by sliding this study window all along the year in order to catch the worst sequences for the system which. This sequence is found easily because it is the lowest ratio of all the possible sequences. Of course, the position of the sequence in the year depends on the duration of this one. The worst 2-day period is found in February while the worst 7-day period occurs in March.

In order to assess which period duration has finally to be considered for the case study, the system is optimized, and its cost evaluated for each worst period duration varying from 1 day to 14 days. Each simulation has been done 5 times and *Figure 6* shows the maximum, the minimum, and the average cost.

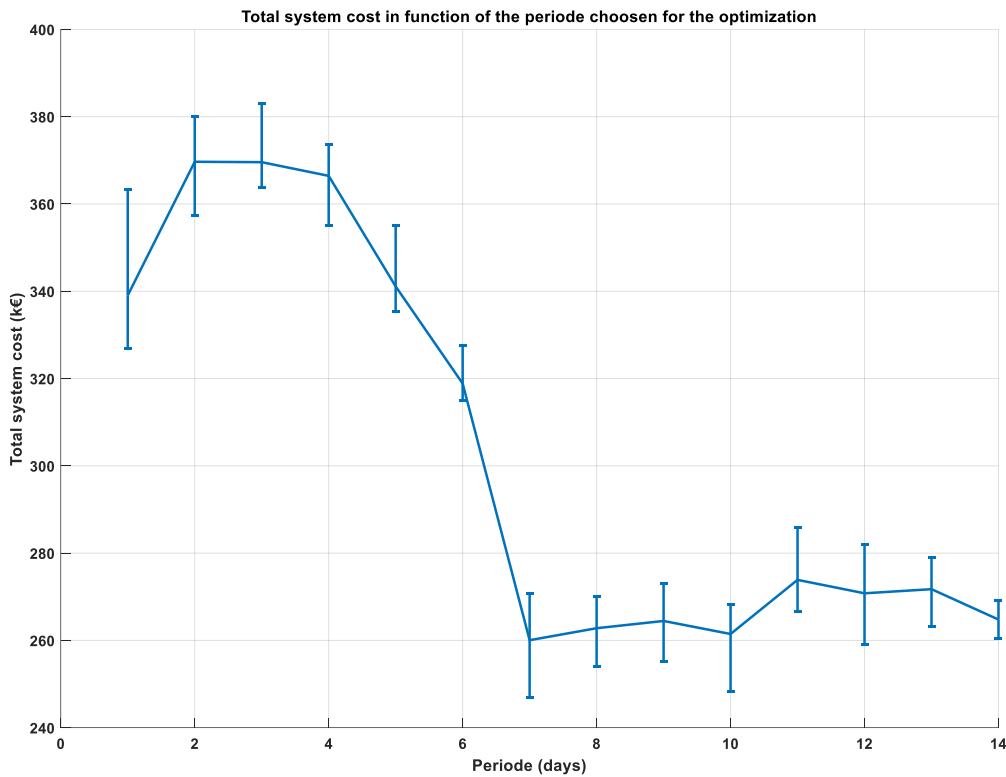


Figure 6 : Total system cost in function of the duration of the worst period

Figure 6 shows that a period lasting more than 7 days is appropriate to size the system in order to minimize its cost. Nevertheless, the shorter is the period the shorter is the computation time due to the size of the optimization variable α which is proportional to the number of optimization points. For a seven days optimization, the number of optimization variables is 170.

One could also wonder why the whole system costs less for a 1-day optimization period than a 2-day period. This could be explained by the fact that the area of PV panels decreases with the increase of the worst period duration because the mean solar irradiation is rising when considering more and more days. *Figure 7* shows the price of PV panels in function of the duration of the worst period. Nevertheless, once the PV area is fixed, there will be more energy to store on sunny days, so the storage cost is increasing at the beginning as shown on *Figure 8* representing the total storage cost that impacts more the overall cost than the PV implemented area.

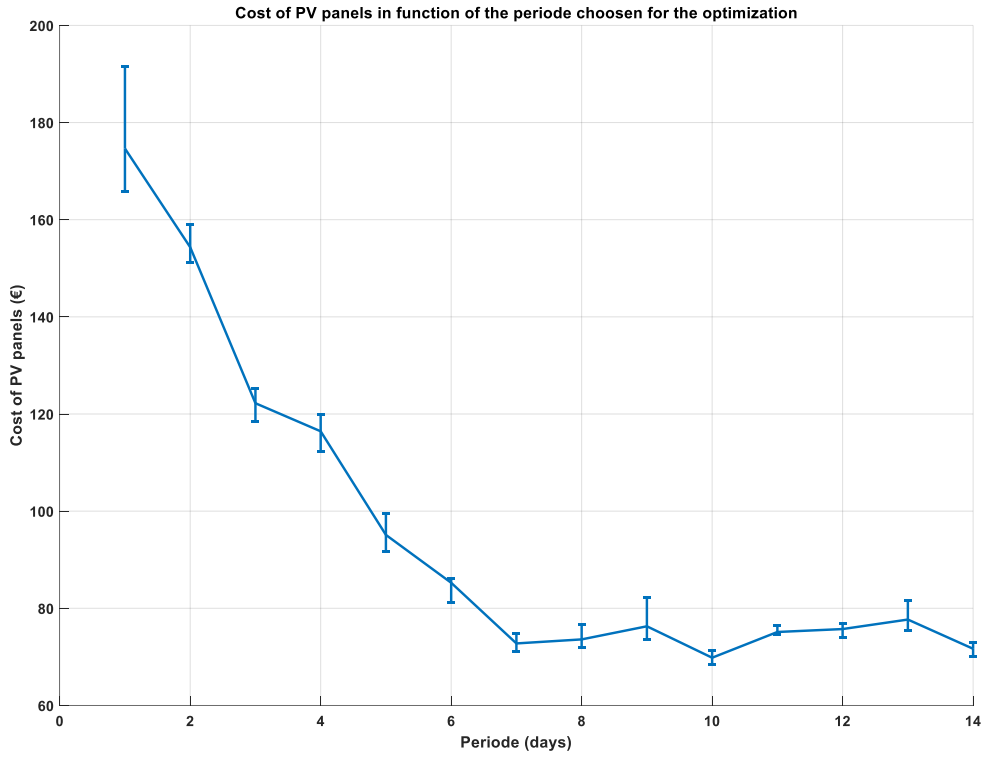


Figure 7 : PV cost evolution as a function of the duration of the worst period

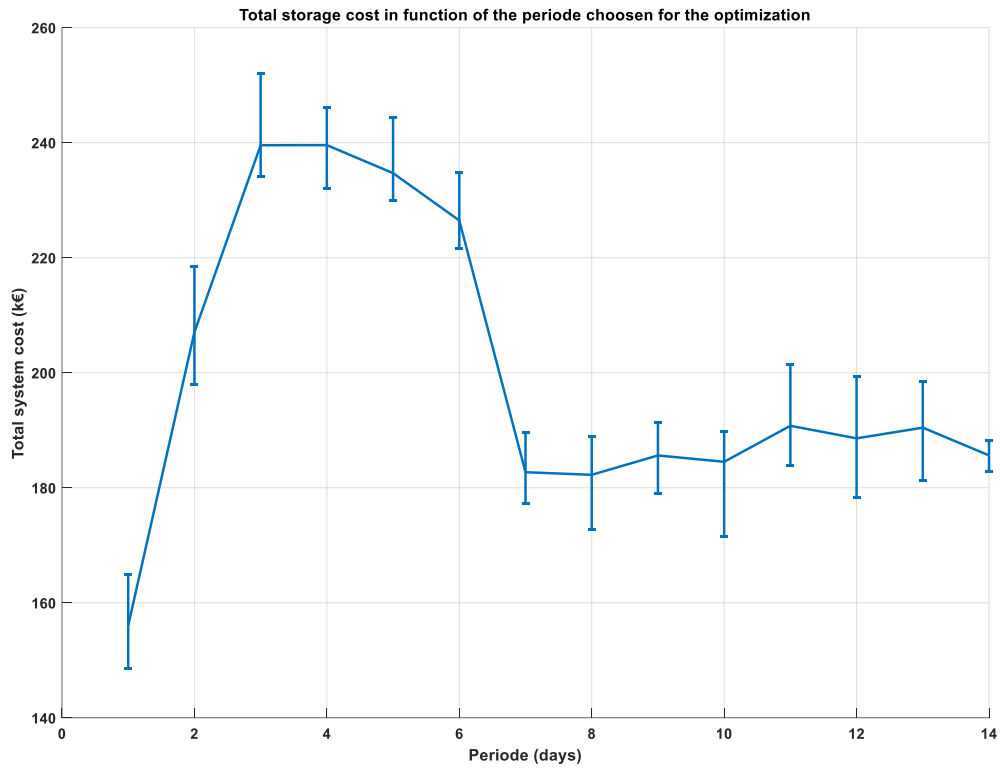


Figure 8 : Storage cost evolution as a function of the duration of the worst period

Figure 9 shows the worst 7-day period of the year according to the ratio presented above. The system will then be sized on this precise week, which start on 3rd November.

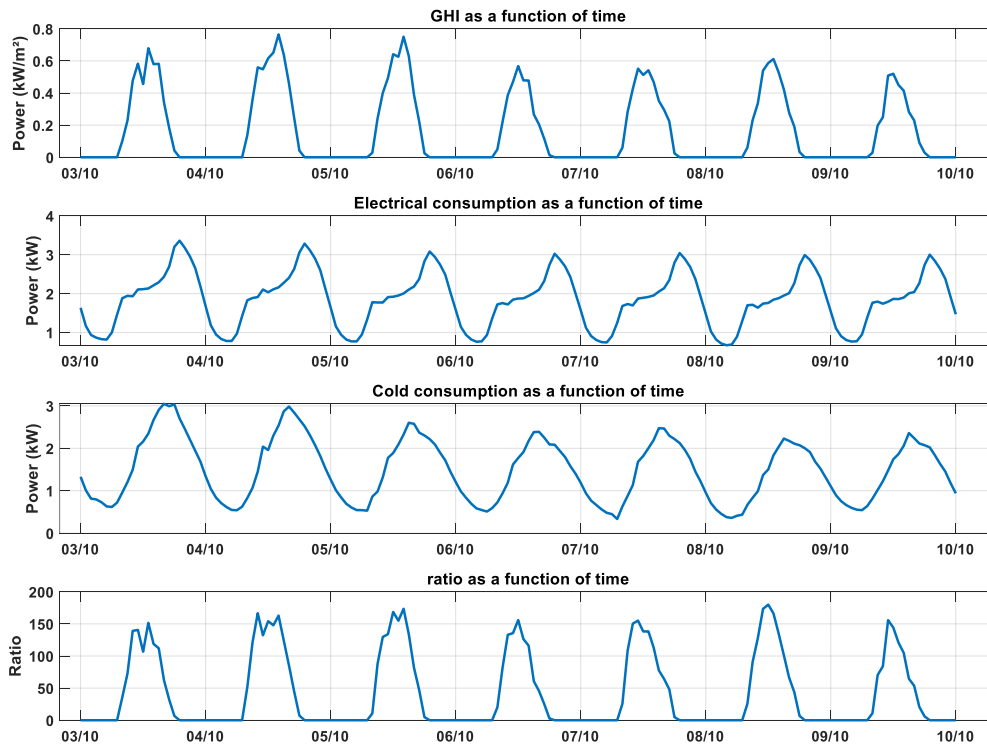


Figure 9 : Data for a residential building during the worst 7 days period of the year

4.3. Results of the case study

The algorithm can give an approximate size for each component in a very short time (few minutes) and the driving strategy to manage the system. Table 3 gives the different sizes and costs of the components and Figure 10 shows the cost repartition between the different components of the system.

Component	Size	Approximate price
Photovoltaic panels	168m ²	71k€
Heat pump	600W	2k€
Electrolyzer	17kW	103k€
Fuel cell	3,7kW	48k€
Hydrogen storage	78,2kWh	12k€
Electrochemical batteries	2kWh	5k€
Thermochemical system	8,8kWh	15k€
		Total : 258k€

Table 3: Sizes and costs of system components.

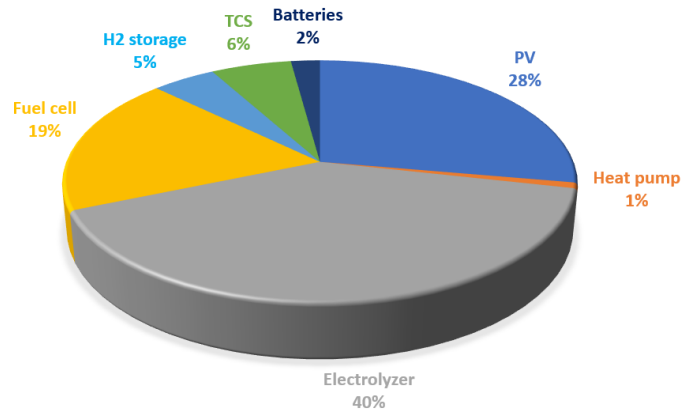


Figure 10 : Cost repartition between the system components.

The major part of the cost (64 %) is due to the storage inside hydrogen. One can also notice that around 168m² of photovoltaic panels are needed, which represent an installed power about 25kW. The price of the system over its lifetime is about 258k€. As a reminder, this building has an electricity consumption about 1 180kWh per month and 860kWh for the cold.

Figure 11 shows, on the positive side of the graph, the power delivered over time by the electrical producers: the photovoltaic panels in orange and the fuel cell in blue. As expected, the fuel cell is only providing electricity at night or when there is not enough PV production. On the negative side of the graph are presented the power consumed over time by the building in green, the heat pump in purple and the electrolyzer in yellow. Once again, the electrolyzer comes into operation only when there is enough PV production. Finally, considering the envelopes of the positive and negative sides it can be asserted that the electricity production is always matching the consumption which means that the optimization algorithm works properly.

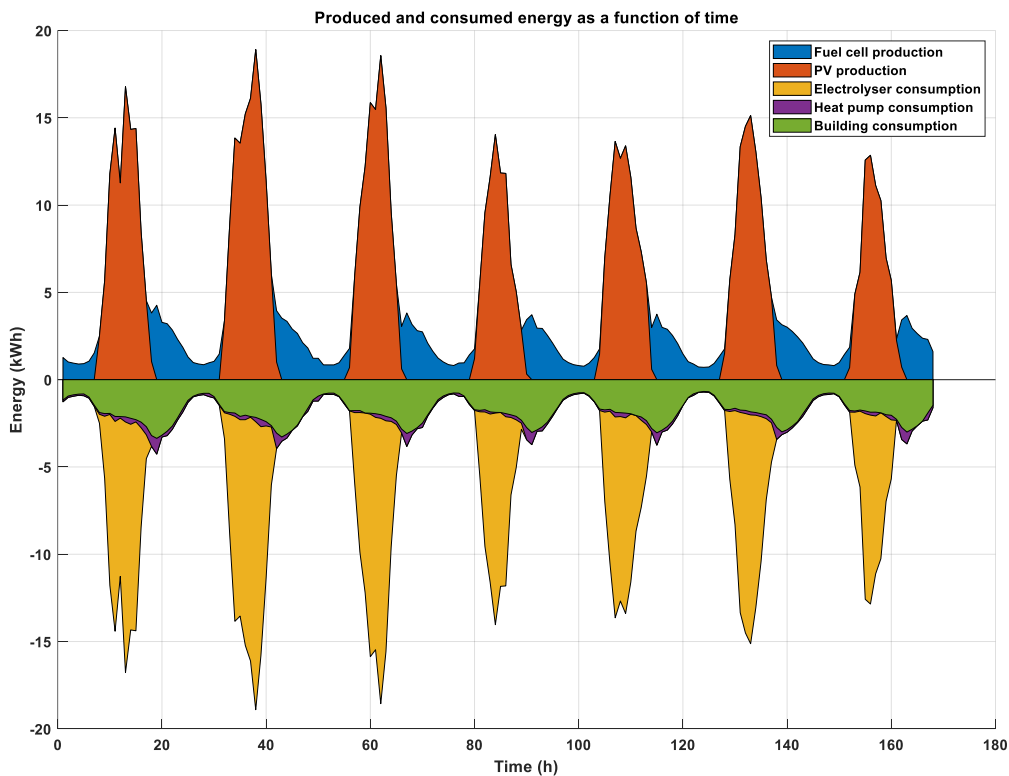


Figure 11 : Temporal distribution of the electrical power inside the system.

In the same way as the previous graph, the *Figure 12* shows the distribution of the cold production on the positive side between the heat pump in yellow and the two thermochemical units in blue and orange. Here again, looking at the envelopes, the production is always well matching the consumption. One can also noticed than the TCS unit provide 46% of the required cold energy which is not negligible.

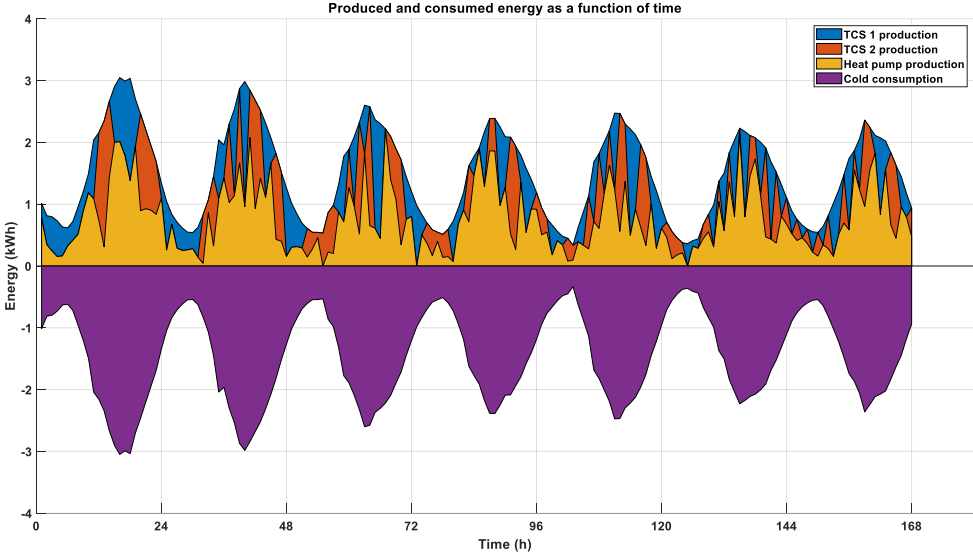


Figure 12: Temporal distribution of the cold power inside the system.

Finally, the evolution of hydrogen in the tank in term of energy during these 7 days is presented in *Figure 13*. This graph is based on equation (7) described earlier. The criterion about the return to initial state at the end of the simulation is fulfilled which corroborate the fact that the algorithm if running properly. This graph can also give the needed quantity of hydrogen, about 80kWh here, which represent around 2,3kg of hydrogen.

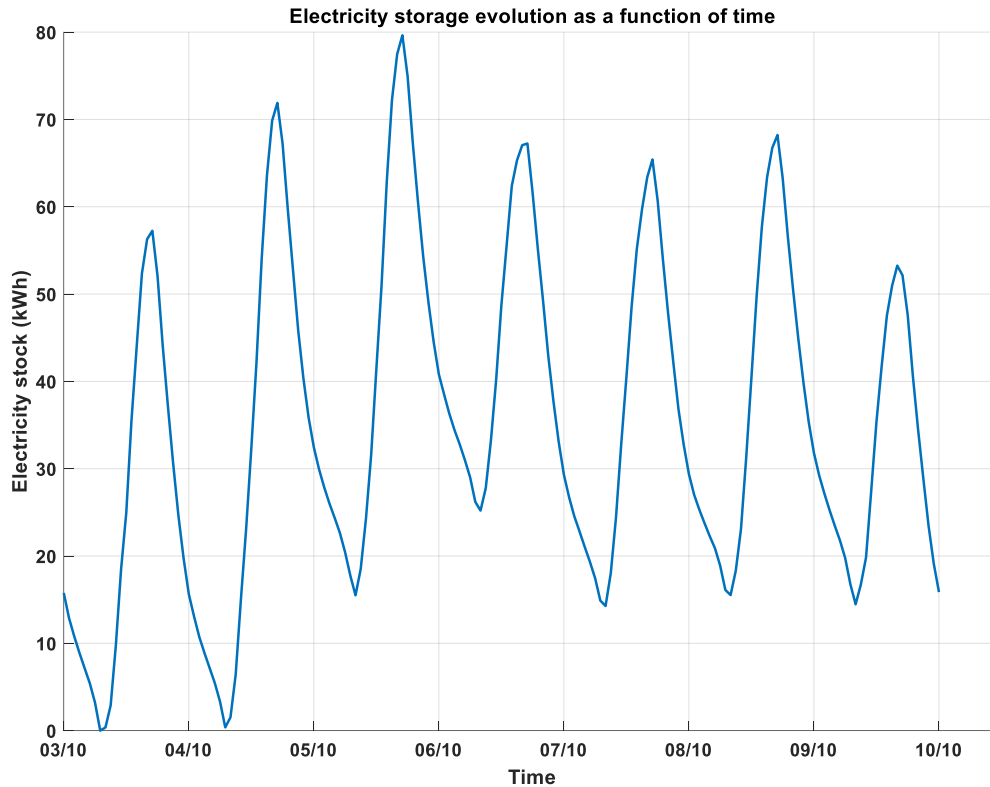


Figure 13: Temporal distribution of the energy stored in the hydrogen tank.

5. Impact of the load profiles on the cost of the whole system

This part is dedicated to a discussion about the evolution of the economic interest of the system as a function of the load profiles. At first, two systems without TCS will be compared in order to see which profiles are more suitable for a storage inside hydrogen instead of electrochemical batteries. Then, the cost of a system with and without the TCS unit when hydrogen is used, will be discussed according to different load profiles.

These studies have been carried out considering 7 different cold profiles and 7 different electrical profiles. This enables the study of 49 different energy building demand profiles. The daily average consumption of cold and electricity has been kept constant in every profile: 48kWh per day have been considered for the electricity consumption. The average cold consumption has been chosen according to [22] where it is said that 36% of the electricity consumption is due to air conditioning. For ease of reference, *Figure 4* shows the different profiles only for 3 different cold and electrical profiles, giving thus 9 profiles in all instead of 49. The horizontal axis represents the repartition of electricity consumption during the day in comparison to the electricity consumption during the night. On the left of this axis there is two times more consumption during the night period than during the day (ratio of 1/2), then moving towards the right there is a constant consumption (ratio of 1) and finally two times more electrical consumption during the day than during the night (ratio of 2). Similarly, the vertical axis represents the repartition of the cold energy consumption between day and night. To give an idea, the previous set of data had a mean electricity ratio about 1.2 and an average cold ratio of 1.8. Both demands were then more during the day than the night.

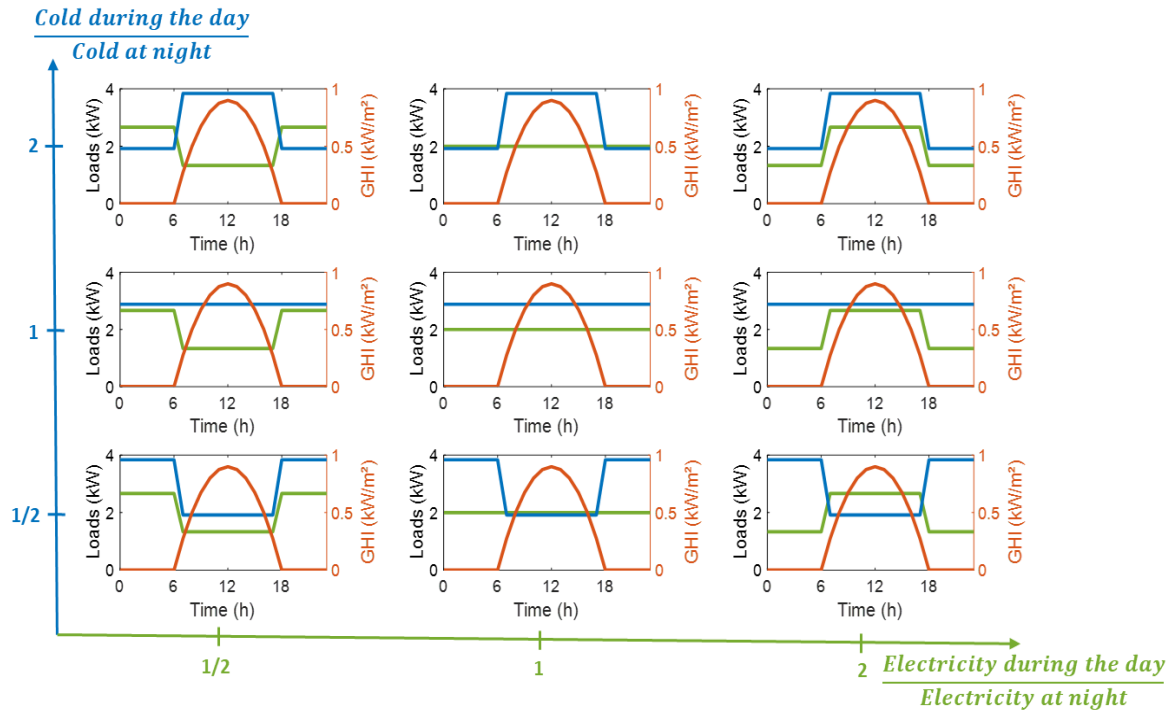


Figure 14: Presentation of 9 of the 49 load profiles used for the studies.

5.1. Interest of a hydrogen storage according to the load profiles

The first study concerns a comparison between an electrical storage into electrochemical batteries and into hydrogen. These two cogeneration systems have been optimized with the PSO algorithm in order to find their approximate costs, according to the 49 different load profiles. In this study, it is no more question of implementing a thermochemical unit. It is then assumed that the cold production is only handled by the electrically driven heat pump.

The system with electrochemical batteries is depicted in *Figure 15*. In this system, the electrical production is handled by photovoltaic panels and the cold production is done by the heat pump. The storage of electrical energy is done by means of electrochemical batteries. To increase battery lifetime, an usual depth of discharge of 50% has been considered for the optimization [39]. This means that twice the capacity really needed should be installed and this has to be considered in the total system cost.

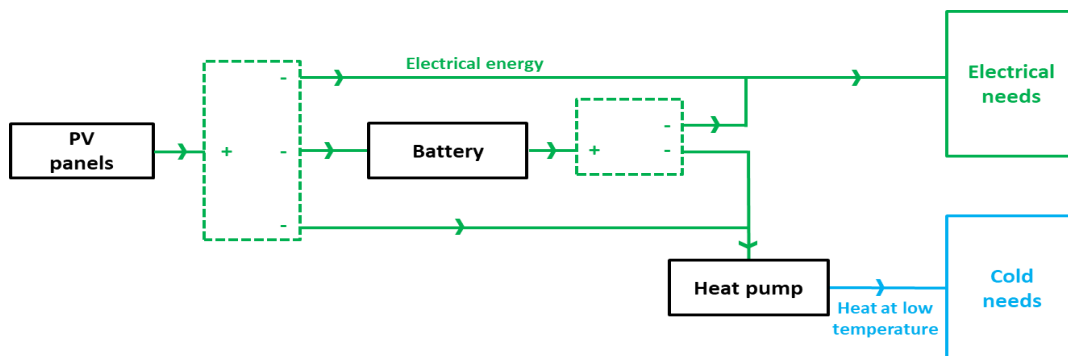


Figure 15: Scheme of the system with an electrical storage inside electrochemical batteries.

The system which stores electricity into hydrogen is depicted in *Figure 16*. As one can see, there are still batteries inside the system, but there are only here to deal with the high dynamic of the system, the power peaks for example. As the algorithm is working with a time step of one hour it is not possible to have an overview of the management of the batteries. That is why only 2kWh of batteries has been considered which seems a quite

reasonable amount of such a system. These batteries will not be considered in the optimization but will nevertheless impact the total cost.

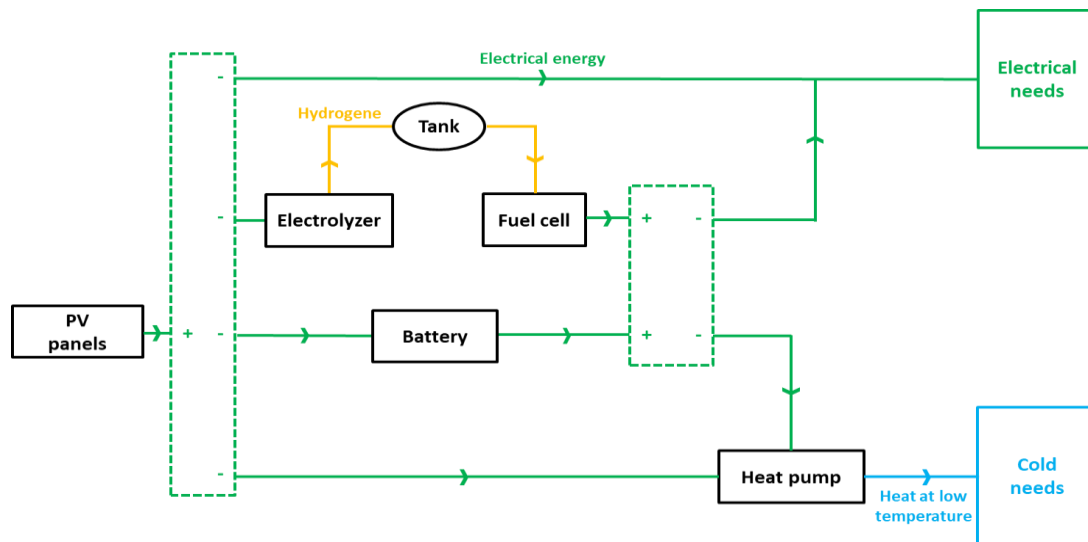


Figure 16: Scheme of the system with an electrical storage thanks to hydrogen.

The results of this study are presented in the *Table 4* which present the cost reduction when hydrogen is used instead of electrochemical batteries. The result is negative when it is more interesting to use hydrogen. To increase understanding, a color coding has been implemented: the greener it is, the more there is an economic interest to use hydrogen. The first thing to notice is that hydrogen is always more interesting than electrochemical batteries in this study because all the results are negative. This result must be treated with caution because it is highly dependent on the considered component costs. For example, in a region where electrochemical batteries are very cheap the conclusion could be different. Nevertheless, the interest of this work is not to arbitrate whether hydrogen is more interesting than batteries or not. The interest is to detect a trend to see if the load profiles have an impact on the economic interest to use hydrogen instead of batteries. Indeed, whatever the cold ratio, the benefits remain quite constant but the more there is electricity to produce at night the more it became interesting to use hydrogen. This can be explained by the size of the battery pack which is directly proportional to the amount of energy to store while, with a hydrogen storage, once an electrolyzer and a fuel cell have been chosen according to the maximum powers involved in the system. The more there is energy to store the more the hydrogen tank must be bigger while the electrolyzer and the fuel cell remain with the same size. As the cost to store the same amount of energy in a hydrogen tank is cheaper than to store it into electrochemical batteries, it become obvious that the more energy there is to store the more it become interesting to use hydrogen instead of batteries. The last thing to notice is that the table is not uniform, this can be explained by the fact that the PSO algorithm can give sub-optimal solutions for some simulations. To decrease this issue, each scenario has been simulated 10 times in order to take the average value.

		Electricity ratio day / night						
		1/4	1/3	1/2	1	2	3	4
Cold ratio day / night	4	-21%	-20%	-19%	-16%	-17%	-16%	-16%
	3	-21%	-20%	-19%	-16%	-17%	-17%	-16%
	2	-22%	-21%	-19%	-17%	-17%	-17%	-16%
	1	-24%	-22%	-21%	-18%	-17%	-17%	-17%
	1/2	-25%	-24%	-21%	-18%	-16%	-17%	-17%
	1/3	-25%	-25%	-23%	-19%	-17%	-16%	-17%
	1/4	-26%	-24%	-24%	-18%	-16%	-16%	-17%

Table 4: Resulting cost reduction by using hydrogen instead of electrochemical batteries.

5.2. Interest of a thermochemical unit according to the load profiles

Using the same 49 load profiles, the PSO algorithm has been used to see when it is interesting to insert a thermochemical unit when hydrogen is used to store electricity. The cost reduction between the systems with and without thermochemical unit are shown in the *Table 5*. The result is negative when it became economically interesting to insert a thermochemical unit in the system.

		Electricity ratio day / night						
		1/4	1/3	1/2	1	2	3	4
Cold ratio day / night	4	7%	8%	8%	4%	9%	8%	9%
	3	7%	6%	6%	3%	7%	8%	8%
	2	5%	4%	4%	3%	2%	6%	7%
	1	2%	2%	4%	2%	0%	3%	4%
	1/2	1%	1%	1%	0%	-1%	-1%	2%
	1/3	1%	1%	1%	0%	-1%	-3%	-1%
	1/4	1%	0%	0%	-2%	-2%	0%	-1%

Table 5: Resulting cost reduction by the addition of a thermochemical unit in the system.

Looking at this table it can be concluded that what matters here is the cold ratio. Whatever the electricity ratio, it becomes interesting to have a thermochemical unit in the system if there is a night consumption of cold. Nevertheless, one should notice that profits are not very interesting, about 3% in the most favorable case. This can be explained by the fact that thermochemical systems are still quite expensive because there are not still widespread in the industry. The interest of adding a thermochemical unit is not much the economic aspect, but rather the environmental aspects because the heat retrieving increase the system efficiency.

To emphasize these conclusions, the *Table 6* shows the direct comparison between a system where electricity is stored thanks to electrochemical batteries and where it is stored in hydrogen with a heat retrieving thanks to a thermochemical unit. As expected, it becomes interesting to use such a system when both consumptions occur at night.

		Electricity ratio day / night						
		1/4	1/3	1/2	1	2	3	4
Cold ratio day / night	4	-15%	-14%	-12%	-12%	-10%	-10%	-8%
	3	-16%	-15%	-14%	-14%	-12%	-10%	-9%
	2	-18%	-17%	-16%	-14%	-15%	-12%	-11%
	1	-23%	-20%	-18%	-16%	-16%	-15%	-14%
	1/2	-24%	-23%	-20%	-18%	-17%	-18%	-16%
	1/3	-25%	-24%	-22%	-19%	-17%	-19%	-18%
	1/4	-25%	-24%	-24%	-19%	-17%	-17%	-17%

Table 6: Resulting cost reduction by using hydrogen storage and a thermochemical unit instead of only electrochemical batteries.

In order to explain more deeply where the cost reductions come from, the *Figure 17* shows the cost repartition for three extreme load profiles: the one with night consumptions (ratio $\frac{1}{4}$), the one with constant consumption (ratio 1) and the one with consumption during the day (ratio 4). For each scenario of consumption, 3 systems are compared : the one with hydrogen and a thermochemical system, the one with hydrogen but without heat retrieving thanks to the TCS and the one with electrochemical batteries and no TCS.

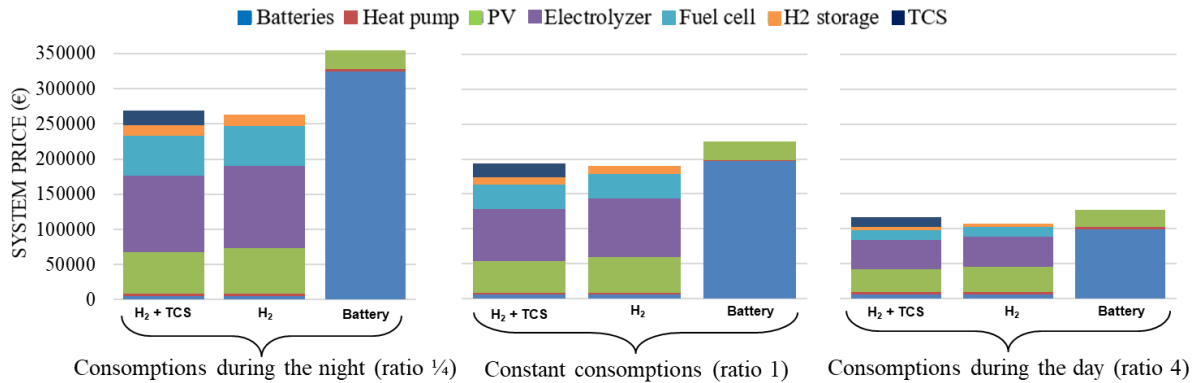


Figure 17: Cost repartition between components for the 3 cogeneration systems and for 3 extremes load profiles.

The first thing to notice is that the more there is energy to store the more the system is expensive whatever the storage used. Another interesting thing to remark is the reduction of the cost of the PV panels as well as the cost of the electrolyzer and the fuel cell when a thermochemical unit is added. Indeed, this cost reduction can be explained by the fact that in the case of night consumptions the PV area is reduced from 150m² to 127m² if a thermochemical unit is installed. This means that the global efficiency has been improved. For a daily production of 50kWh of electricity and 72kWh of cold, 150m² of PV panels produce around 160kWh of electricity for one day against 136kWh for 127m².

6. Conclusion and perspectives

The conception of a particle swarm optimization algorithm able to optimize at the same the component sizes and the driving strategy of cogeneration systems of cold and electricity has brought several achievements.

First, a method to apply the algorithm on different sets of data has been shown. The key point is to find the worst scenario occurring during the year to size our stand-alone system. Once the duration of the worst period found, the algorithm has shown its capacity to find accurate solution in a small computation time. For the record, this system will use photovoltaic panels to produce electricity to deliver electricity to a building. The excess of electricity is stored in hydrogen thanks to an electrolyzer and a fuel cell is used to prevent for the shortage. The building climatization is ensured by an electrically driven heat pump assisted by a thermochemical system which retrieve the low-grade heat from the electrolyzer and the fuel cell.

Another achievement has been to show that the more the electricity is consumed at night the more it become interesting to use a hydrogen-based storage instead of electrochemical batteries. This result remaining correct whatever the cold load profile. Nevertheless, one must keep in mind that this work concludes only about the trend because depending on the costs taking into account it could be possible that even with night consumption, electrochemical batteries remain cheaper than a hydrogen-based storage.

The last achievement of this work concerns the addition of a thermochemical unit in the system, the economic profit has not been proven, but if cold consumption occurs at night, a more efficient system can be designed for approximately the same cost. Such interesting profiles for a cogeneration system with hydrogen and thermochemical unit could be found in hospital, museum, hotels where occur a night consumption of cold and electricity.

The system of cogeneration studied in this paper could be improved in the future to design a trigeneration system of electricity, cold and heat. Further studies can also be carried out by investigating other cold applications such as refrigeration or even deep-freezing applications.

Acknowledgments

This work has been financially supported by the French National Research Agency (ANR) in the framework of the RECIF project under contract ANR-18-CE05-0043 (<https://anr.fr/Projet-ANR-18-CE05-0043>). The authors are also thankful to Prof. Franck Lucas from the GEPASUD laboratory for his help on having data to work with. The authors are also grateful to Prof. Daniel Hissel and Dr. Samir Jemei from the FC-Lab (FEMTO Laboratory) for their fruitful discussions and advises they provide us about fuel cell technology. These studies have been conducted within the PROMES laboratory which the authors would like to thank too.

References

- [1] T. Taner, "Energy and exergy analyze of PEM fuel cell: A case study of modeling and simulations," *Energy*, 2018.
- [2] B. Shabani, J. Andrews, and S. Watkins, "Energy and cost analysis of a solar-hydrogen combined heat and power system for remote power supply using a computer simulation," *Sol. Energy*, 2009.
- [3] B. Shabani and J. Andrews, "An experimental investigation of a PEM fuel cell to supply both heat and power in a solar-hydrogen RAPS system," *Int. J. Hydrogen Energy*, 2011.
- [4] F. A. Al-Sulaiman, I. Dincer, and F. Hamdullahpur, "Energy analysis of a trigeneration plant based on solid oxide fuel cell and organic Rankine cycle," *Int. J. Hydrogen Energy*, 2010.
- [5] V. Palomba, M. Ferraro, A. Frazzica, S. Vasta, F. Sergi, and V. Antonucci, "Experimental and numerical analysis of a SOFC-CHP system with adsorption and hybrid chillers for telecommunication applications," *Appl. Energy*, vol. 216, no. October 2017, pp. 620–633, 2018.
- [6] M. V. Oro, R. G. de Oliveira, and E. Bazzo, "An integrated solution for waste heat recovery from fuel cells applied to adsorption systems," *Appl. Therm. Eng.*, vol. 136, no. August 2017, pp. 747–754, 2018.
- [7] P. Margalef and S. Samuelsen, "Integration of a molten carbonate fuel cell with a direct exhaust absorption chiller," *J. Power Sources*, vol. 195, no. 17, pp. 5674–5685, 2010.
- [8] Z. Yu, J. Han, and X. Cao, "Investigation on performance of an integrated solid oxide fuel cell and absorption chiller tri-generation system," *Int. J. Hydrogen Energy*, vol. 36, no. 19, pp. 12561–12573, Sep. 2011.
- [9] E. Baniasadi and A. A. Alemrajabi, "Fuel cell energy generation and recovery cycle analysis for residential application," *Int. J. Hydrogen Energy*, vol. 35, no. 17, pp. 9460–9467, 2010.
- [10] V. Palomba, M. Prestipino, and A. Galvagno, "Tri-generation for industrial applications: Development of a simulation model for a gasification-SOFC based system," *Int. J. Hydrogen Energy*, vol. 42, no. 46, pp. 27866–27883, 2017.
- [11] M. Mehrpooya, S. Sayyad, and M. J. Zonouz, "Energy, exergy and sensitivity analyses of a hybrid combined cooling, heating and power (CCHP) plant with molten carbonate fuel cell (MCFC) and Stirling engine," *J. Clean. Prod.*, vol. 148, pp. 283–294, 2017.
- [12] K. F. Fong and C. K. Lee, "Investigation on zero grid-electricity design strategies of solid oxide fuel cell trigeneration system for high-rise building in hot and humid climate," *Appl. Energy*, vol. 114, pp. 426–433, 2014.
- [13] C. Weber, F. Maréchal, D. Favrat, and S. Kraines, "Optimization of an SOFC-based decentralized polygeneration system for providing energy services in an office-building in Tōkyō," *Appl. Therm. Eng.*, vol. 26, no. 13, pp. 1409–1419, 2006.
- [14] S. Ma, J. Wang, Z. Yan, Y. Dai, and B. Lu, "Thermodynamic analysis of a new combined cooling, heat and power system driven by solid oxide fuel cell based on ammonia-water mixture," *J. Power Sources*, vol. 196, no. 20, pp. 8463–8471, 2011.
- [15] F. Calise, G. Ferruzzi, and L. Vanoli, "Transient simulation of polygeneration systems based on PEM fuel

- cells and solar heating and cooling technologies,” *Energy*, vol. 41, no. 1, pp. 18–30, 2012.
- [16] X. Chen, G. Gong, Z. Wan, L. Luo, and J. Wan, “Performance analysis of 5 kW PEMFC-based residential micro-CCHP with absorption chiller,” *Int. J. Hydrogen Energy*, vol. 40, no. 33, pp. 10647–10657, Sep. 2015.
- [17] M. Martins, S. Mauran, D. Stitou, and P. Neveu, “A new thermal-hydraulic process for solar cooling,” *Energy*, vol. 41, no. 1, pp. 104–112, 2012.
- [18] B. Michel, N. Mazet, S. Mauran, D. Stitou, and J. Xu, “Thermochemical process for seasonal storage of solar energy: Characterization and modeling of a high density reactive bed,” *Energy*, vol. 47, no. 1, pp. 553–563, 2012.
- [19] D. Stitou, N. Mazet, and S. Mauran, “Experimental investigation of a solid/gas thermochemical storage process for solar air-conditioning,” *Energy*, vol. 41, no. 1, pp. 261–270, 2012.
- [20] F. Ferrucci, D. Stitou, P. Ortega, and F. Lucas, “Mechanical compressor-driven thermochemical storage for cooling applications in tropical insular regions. Concept and efficiency analysis,” *Appl. Energy*, vol. 219, no. December 2017, pp. 240–255, 2018.
- [21] N. Le Pierrès, D. Stitou, and N. Mazet, “New deep-freezing process using renewable low-grade heat: From the conceptual design to experimental results,” *Energy*, vol. 32, no. 4, pp. 600–608, 2007.
- [22] T. SOFRES, “Etude du niveau d’équipement et des comportements des ménages à Tahiti et Moorea en matière d’énergie : étude par sondage,” 2011.
- [23] ADEME, “Plan climat-énergie de la polynésie française,” 2015.
- [24] E. Elbeltagi, T. Hegazi, and D. Grierson, “Comparison among five evolutionary-based optimization algorithms,” *Adv. Eng. Informatics*, vol. 19, no. 1, pp. 43–53, Jan. 2005.
- [25] D. E. Goldberg and J. H. Holland, “Genetic Algorithms and Machine Learning,” *Mach. Learn.*, vol. 3, no. 2/3, pp. 95–99, 1988.
- [26] J. Kennedy and R. Eberhart, “Particle swarm optimization,” in *Proceedings of ICNN’95 - International Conference on Neural Networks*, vol. 4, pp. 1942–1948.
- [27] S. Das, A. Abraham, and A. Konar, *Particle Swarm Optimization and Differential Evolution Algorithms: Technical Analysis, Applications and Hybridization Perspectives*, no. May 2014. 2008.
- [28] S. Twaha and M. A. M. Ramli, “A review of optimization approaches for hybrid distributed energy generation systems: Off-grid and grid-connected systems,” *Sustain. Cities Soc.*, vol. 41, no. April, pp. 320–331, 2018.
- [29] A. Stoppato, A. Benato, N. Destro, and A. Mirandola, “A model for the optimal design and management of a cogeneration system with energy storage,” *Energy Build.*, vol. 124, pp. 241–247, 2016.
- [30] J. Wang, Z. J. Zhai, Y. Jing, and C. Zhang, “Particle swarm optimization for redundant building cooling heating and power system,” *Appl. Energy*, 2010.
- [31] H. Anand, N. Narang, and J. S. Dhillon, “Multi-objective combined heat and power unit commitment using particle swarm optimization,” *Energy*, 2019.
- [32] S. Singh, P. Chauhan, and N. J. Singh, “Capacity optimization of grid connected solar/fuel cell energy system using hybrid ABC-PSO algorithm,” *Int. J. Hydrogen Energy*, vol. 45, no. 16, pp. 10070–10088, 2020.
- [33] J. Cot-Gores, A. Castell, and L. F. Cabeza, “Thermochemical energy storage and conversion: A-state-of-the-art review of the experimental research under practical conditions,” *Renew. Sustain. Energy Rev.*, vol. 16, no. 7, pp. 5207–5224, Sep. 2012.
- [34] “Hawai data on residential households,” 2017. [Online]. Available: https://openei.org/datasets/files/961/pub/EPLUS_TMY2_RESIDENTIAL_BASE/.
- [35] R. Hendron and C. Engebrecht, “Building America House Simulation Protocols,” no. October, p. 79, 2010.
- [36] A. Brka, “Optimisation of stand-alone hydrogen-based renewable energy systems using intelligent techniques Optimisation of stand-alone hydrogen-based renewable energy systems using intelligent techniques,” 2015.
- [37] N. S. Attemene, K. S. Agbli, S. Fofana, and D. Hissel, “Optimal sizing of a wind, fuel cell, electrolyzer,

- battery and supercapacitor system for off-grid applications,” *Int. J. Hydrogen Energy*, no. xxxx, 2019.
- [38] K.-P. Kairies, “Battery storage technology improvements and cost reductions to 2030: A Deep Dive,” *Int. Renew. Energy Agency Work.*, 2017.
- [39] B. University, “How to Prolong Lithium-based Batteries,” 2019. [Online]. Available: https://batteryuniversity.com/learn/article/how_to_prolong_lithium_based_batteries.